FUNDAMENTAL STUDIES OF NEURAL STIMULATING ELECTRODES

Seventh Quarterly Report
Covering Period February 29, 1996 to May 28, 1996
CONTRACT NO. N01-NS-4-2310

T. L. Rose
S. F. Cogan
U. M. Twardoch
G. S. Jones
R. B. Jones
Y. P. Liu

EIC Laboratories, Inc.
111 Downey Street
Norwood, Massachusetts 02062

Prepared for

National Institutes of Health
National Institute of Neurological
Disorders and Stroke
Bethesda, Maryland 20892

July, 1996

This QPR is being sent to you before it has been reviewed by the staff of the Neural Prosthesis Program.

TABLE OF CONTENTS

Section	Page
1 INTRODUCTION AND SUMMARY	6
2 VOLTAMMETRIC STUDIES ON IR MICROELECTRODES	8
2.1 Michigan Ribbon Cable Probe No. 1, Site 1	8
2.2 Michigan Ribbon Cable Probe 4, Site 5	17
3 ELECTRODES WITH GRADED IR/IR INTERFACES	22
3.1 Preparation of Ir/Ir Films by Sputter Deposition	22
3.2 Electrochemical Test Protocol	24
3.3 Electrodes with Discrete Ir/Ir Interface and 75 nm Ir Films	26
3.4 Electrodes with Graded Ir/Ir Interface and 75 nm Ir Films	29
3.5 Electrodes with Discrete Ir/Ir Interface and 100 nm Ir Films	31
3.6 Electrochemistry of Sputtered Ir Films Cycled in PBS	32
4 WORK FOR NEXT QUARTER	37
5 REFERENCES	38

LIST OF FIGURES

Page

Figure 2.1 Schematic representation of U. Michigan ribbon cable probe and numbering scheme for the electrode sites 8

Figure 2.2 Apparent capacitance of site 1 on U. Michigan ribbon cable probe No. 1 at 200 V/s for the eighteen scan rate studies 10

Figure 2.3 Voltammograms of site 3 (top) and 4 (bottom) of the U. Michigan ribbon cable No. 1 after 121 days of passive soaking 12

Figure 2.4 Voltammograms of site 6 (top) and 2 (middle) and 5 (bottom) of the U. Michigan ribbon cable No. 1 after 121 days of passive soaking 14

Figure 2.5 Top: Voltammograms of site 1 of the U. Michigan ribbon cable No. 1 after [illegible] days of passive soaking 15

Figure 2.6 Comparison of wide potential cyclic voltammograms for U. Michigan ribbon cable probe No. 4, site 5 before and after scan rate study 18

Figure 2.7 Plot of C_{app} as function of sweep rate for site 5 on ribbon No. 4 taken in PBS during the Ru studs 19

Figure 2.8 Voltammograms of U. Michigan ribbon cable probe no. 4 site 3 at 0.05 V/s in deaerated 0.1M PBS after 60 days soaking 20

Figure [illegible] Schematic diagram of sputter deposition apparatus used to produce graded interfaces in multilayer thin films 23

Figure [illegible] Current versus time profile used to grade the composition of the interface between Ti and Ir in a Ti-Ir electrode on Si 23

Figure [illegible] Cyclic voltammogram of discrete interface Ti-Ir electrode in Ar sparged PBS before and after 240 activation pulses in 0.3 M Na_2HPO_4 25

Figure [illegible] Cyclic voltammograms of discrete interface Ti-Ir electrode (75 nm Ir) taken while the electrode was pulsed over 11520 pulses in Ar sparged PBS 27

Figure [illegible] SEM cross section of AIROF delaminated after pulsing a discrete interface Ti-Ir electrode for 11,520 pulses 28

Figure [illegible] SEM of AIROF surface after delamination following pulsing of a discrete interface Ti-Ir electrode for 11,520 pulses 28

Figure [illegible] Cyclic voltammograms of a graded interface Ti/Ti electrode [illegible] nm Ir over [illegible] pulses in Ar sparged PBS ..... [illegible]

Figure [illegible] Cyclic voltammograms of a discrete interface Ti/Ti electrode [illegible] nm Ir after [illegible] and [illegible] pulses in Ar sparged PBS 33

Figure [illegible] Comparison of cyclic voltammograms of Ti/Ti electrodes showing the occurrence of the wave at 0.6-0.7 V vs. SCE associated with delamination of the AIROF 33

Figure [illegible] Cyclic voltammogram of AIROF showing development of a redox wave at [illegible] V following 18,240 pulses in PBS/Ar 34

LIST OF TABLES

Page

Table 2.1 Current measurements for the scan rate studies on site 1 of 4 Michigan ribbon cable probe No. 4 19

Table 2.2 Data for electrochemical study 1 on site 5 of 4 Michigan ribbon cable probe No. 4 19

Table 2.3 Comparison of dimensions determined from electrochemical testing of sputtered iridium electrodes of Schmidt 2 type on 4 Michigan ribbon cable probes 21

Table 3.1 Conditions for sputter deposition of Ti and Ir films with discrete and graded interfaces on silicon 24

Table 3.2 Results from pulse testing of an electrode (No. 03219677) with a discrete interface between the Ti and a 75 nm Ir film 26

Table 3.3 Results from pulse testing of an electrode (No. 03229035) with a graded interface between the Ti and a 75 nm Ir film 30

Table 3.4 Results from pulse testing of an electrode (No. 05179622) with a discrete interface between the Ti and a 100 nm Ir film 32

Table 3.5 Comparison of Redox Potentials of AIROF on sputtered electrodes with those grown on Ir rods measured at pH 7.3 35

I. INTRODUCTION AND SUMMARY

This report describes the work on NINDS Contract No. N01-NS-4-2330 during the period February 29, 1996 to May 28, 1996. As part of the Neural Prosthesis Program, the broad objectives of the present fundamental studies are: (1) to evaluate the electrochemical processes that occur at the electrode-electrolyte interface during pulsing regimens characteristic of neural prosthetic applications; (2) to establish charge injection limits of stimulation electrode materials which avoid irreversible electrochemical reactions; (3) to develop an *in vitro* method, which can be applied *in vivo*, for determining the electrochemical real area and stability of microelectrodes; (4) to select new materials which can operate at high stimulation charge densities for neurostimulation; and (5) to provide electrochemical and analytical support for other research activities in the Neural Prosthesis Program at NINDS.

Long-term stability studies of a U. Michigan ribbon-cable probe No. 1 have continued for over 200 days. The apparent capacitance of the site calculated from the current at 0.0V vs. Ag/AgCl showed little, if any, increase since the 100th day, indicating **excellent long-term stability of the metal/insulator seal**. On the 171st day, cyclic voltammograms at 0.1 V/s were measured on all sites over a potential window large enough to evaluate the electrochemical properties of the oxide on the sites. The most oxide was observed on the site on which the apparent capacitance measurements were made. Growth in the apparent capacitance prior to the 100th day is attributed to oxide on the electrode. There was evidence of some oxide on three other sites. The source of the oxide is not known. The oxide on the site formed as a result of the electrochemical testing is less resistive than the oxide on the other sites that have been passively soaked. These results suggest that to obtain the best quality oxide, the electrode should be activated either by long-term soaking *in vitro* or *in vivo*.

Examination of two iridium sites on another ribbon cable probe qualitatively showed the same behavior seen on analogous probes. The maximum current at low scan rates in the Ru study, however, was about half that obtained on previous probes resulting in a calculated area about 28% of the geometric area. In contrast, the area based on the apparent capacitance at high sweep rates was comparable to the initial value obtained on site 1, ribbon-cable probe No. 1. After 90 days of soaking the probe, the cyclic voltammograms of all the sites were characteristic

[illegible] electrodes with a good seal at the metal/insulator interface. The small area determined by the [illegible] the area determined by the capacitance so that from the Ru study [illegible] stability of the electrodes, but more measurements on ribbon cable [illegible] confirm the reliability of these diagnostic methods.

[illegible] began studies on graded Ti/Ir bilayers as a method for enhancing the adhesion [illegible] delamination of thin sputtered Ir films if they are overactivated. Graded films were sputtered onto Si substrates by depositing Ti and Ir simultaneously and steadily [illegible] Ti/Ir throughout the layer to form the following structure:

Si/Ti (25 nm), Ti/Ir (50 nm), Ir (75 nm)

Auger analysis determined that the interface was not uniformly graded between the two pure [illegible] resulting in a sharper interface than desired. The films were masked with epoxy to [illegible] an area of about 0.02 cm^2 and the Ir was activated with 240 pulses in inorganic phosphate [illegible] phosphate buffered saline (PBS), pH [illegible]

The electrodes were then subjected to continuous pulsing at potentials large enough to [illegible] additional Ir oxide. The results were compared with 75 nm Ir films that were deposited [illegible] to form a discrete interface. The graded layer electrodes survived over [illegible] pulses before delamination, which was over three times the number that led to [illegible] of the electrodes with the discrete interface. The morphology of the delaminated films [illegible] by SEM showed a dense thin layer on top, which was the initial oxide layer formed, and a thicker porous columnar layer underneath. At intervals throughout the pulsing, the [illegible] of the AIROF layers were measured. The qualitative changes in the [illegible] and graded interface with pulsing were comparable. Heralding the [illegible] sharp growth in the CV of an anodic peak at about 0.6 to 0.7 V vs. SCE and the decrease [illegible] current around 0.2 V vs. SCE associated the reversible Ir(III)/Ir(IV) redox [illegible] electrode with a discrete interface and a 100 nm thick Ir layer was also tested. This film survived [illegible] as many pulses as the graded interface electrode. Until an electrode is tested [illegible] graded interface, therefore, it cannot be determined if the improved pulsing [illegible] graded electrode was due to having an effectively thicker Ir layer or due to the graded [illegible] interface.

2. VOLTAMMETRIC STUDIES ON Ir MICROELECTRODES

During this quarter we continued studies of the long term stability of Ir sites on a probe with an integrated ribbon cable received from U. Michigan. We also evaluated the electrochemical surface area of an additional ribbon cable probe. The integrated ribbon cables allow long term soaking studies without any structures other than those fabricated on the wafer being exposed to the electrolyte solution, which avoids the previous problems with electrolyte penetration beneath the epoxy covering the contact pads. Figure 2.1 is a diagrammatic representation of the probe showing the numbering scheme for the electrode sites.

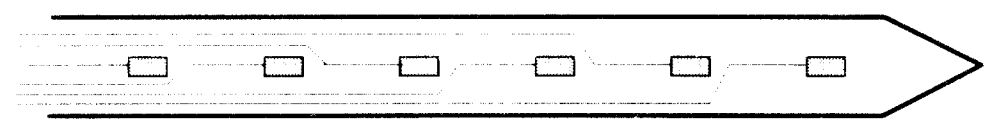

Figure 2.1 Schematic representation of U. Michigan ribbon-cable probe and numbering scheme for the electrode sites.

2.1 U. Michigan Ribbon-Cable Probe No. 1, Site 1.

Electrode Area Measurements. Measurements of the background residual currents on site 1 of U. Michigan ribbon cable probe No. 1 were continued this quarter. Test procedures and results of the first 35 days of electrochemical testing were described in Quarterly Progress Report No. 5 and those of days 35 through 108 were described in Quarterly Progress Report No. 6. This quarter we continued the use of an abbreviated cyclic voltammetry test protocol which was employed to monitor the electrode status during the long term soaking period from 108 to 203 days as described in Quarterly Progress Report No. 6. Briefly, the current is measured at 0.0V vs. Ag/AgCl, when the voltage on the electrode is swept from +0.1V to -0.4V vs. Ag/AgCl in a solution of deaerated 0.1M PBS.

Table 2 lists the background current obtained from the eight studies performed this quarter along with the data from the ten studies conducted during the previous two quarters. Figure 2 lists the apparent capacitance C_{app} at 200 V/s as a function of time. C_{app} is calculated by dividing the current at 0 V vs. Ag/AgCl by the scan rate, thus $C_{app} = Q/V = i/v$, where v is the scan rate.

Table 2 Current measurements for the scan rate studies on site 1 of U. Michigan ribbon-cable probe No. 1

Study No.	Days Soaked	(V/s) = 0.05	10	20	50	100	200
				Current (nA)[1]			
	[illegible]	0.096	6.2	11.0	26.8	45.5	79.5
2	[illegible]	0.138	9.9	18.8	11.6	[illegible]	26
[illegible]	[illegible]	0.142	11.8	21.4	45.0	[illegible]	134
4	[illegible]	0.150	12.4	21.8	48.5	83.5	38
5	[illegible]	0.144	12.3	21.4	46.0	78.5	130
[illegible]	[illegible]	0.148	12.2	21.4	46.0	82.0	129
[illegible]	[illegible]	0.156	11.8	21.2	46.0	82.5	127
[illegible]	[illegible]	0.240	22.0	42.5	110	151	264
[illegible]	[illegible]	0.226	33.0	58.0	128	230	365
	[illegible]	0.334	34.5	63.0	136	246	400
	[illegible]	0.416	44.4	75.0	161	276	430
2	[illegible]	0.446	50.5	86.0	181	318	508
[illegible]	[illegible]	0.446	48.5	85.5	187	332	492
4	[illegible]	0.555	60.5	104.0	222	380	605
5	[illegible]	0.485	48.5	84.5	182	308	485
6	[illegible]	0.610	53.5	95.0	200	344	510
[illegible]	[illegible]	0.525	53.0	91.5	196	328	500
8	[illegible]	0.500	48.0	80.0	168	268	415

[1] Current at 0.0 V vs. Ag/AgCl/5 M NaCl measured from voltammogram taken in PBS

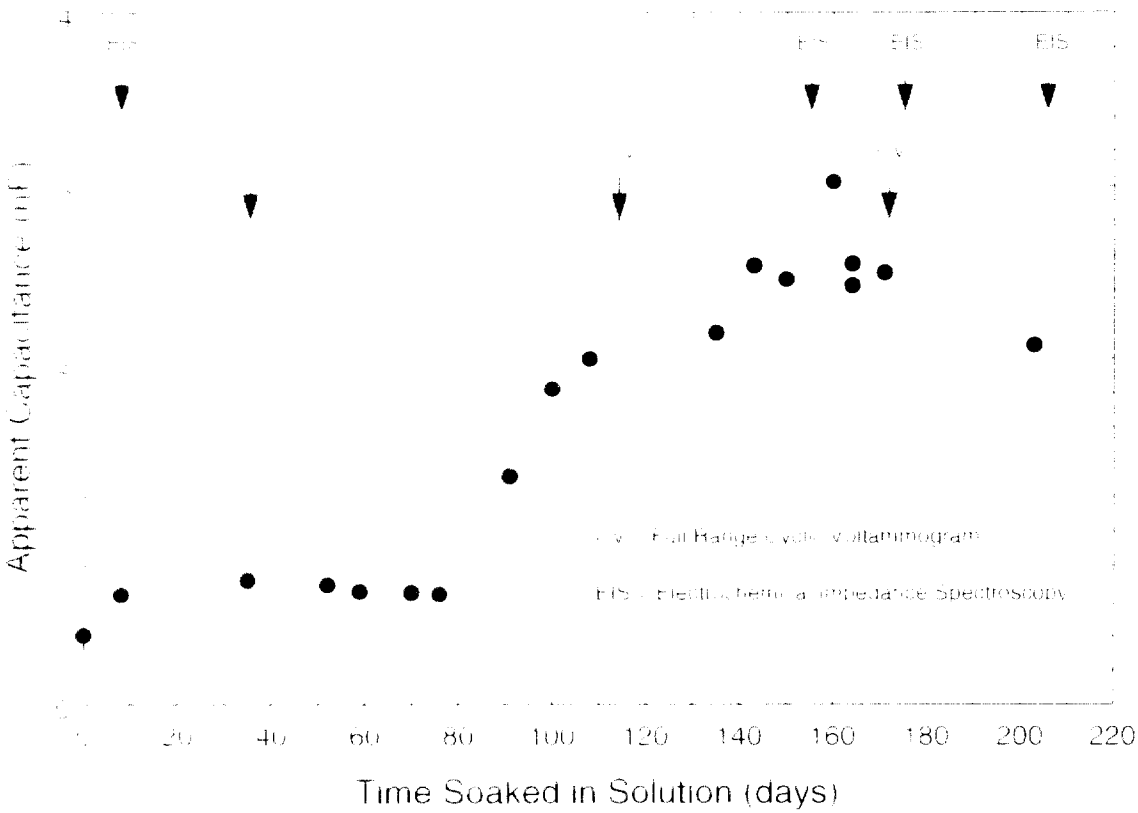

Figure 2.2 Apparent capacitance of site 1 on U. Michigan ribbon-cable probe No. 1 at 200 mV for the EIS scan rate studies. EIS and CV indicate days for measurement of electrochemical impedance spectroscopy and wide potential cyclic voltammetry, respectively.

The apparent capacitance at the high sweep rates on a bare metal electrode should be directly proportional to the real electrochemical surface area. As discussed in Quarterly Progress Report No. [illegible] we have been using 25 μF/cm² real cm² as the proportionality constant based on capacitance values for measurements on Ir wire [1,2]. This value applies to an Ir surface that is perfectly smooth, i.e. has a roughness factor of 1, and the geometric and real surface areas are equal. For an electrode with a higher roughness factor, a larger proportionality constant must be used to replace the geometric area of the electrode. Regardless of the absolute magnitude of the proportionality constant, the increased current leading to the higher apparent capacitance in Figure 2.2 would indicate an increase in area of a bare metal electrode. However, the overall shape of the cyclic voltammograms did not change significantly over the soaking period, the

current at the starting voltage was not anodic, and there was no "tilt" of the voltammogram, all indications of a weak between the metal and insulation layers.

Formation of oxide would also explain the observed increase in the current because the oxide has a specific capacitance many times that of the bare metal, even for very thin films. As is discussed below, measurement of the cyclic voltammogram over the full potential window did show that there was a significant amount of oxide on the electrode. The conclusion to date on this site, therefore, is that there has been little, if any, change in the contact area of the electrolyte with the geometric area of the electrode.

Cyclic Voltammetry Analysis. In order to minimize formation of iridium oxide by electrochemical activation, we have avoided as much as possible taking site 1 of ribbon No. 1 to very high anodic potentials. All of the initial scan rate studies done with Ru at the beginning of the soaking period and all the cyclic voltammogram measurements made to follow changes in the apparent capacitance were limited to potentials between -0.4V and +0.2V vs. Ag/AgCl. During the 118 experiments the electrode was held at potentials between the range of -0.3V and +0.5V vs. Ag/AgCl. Activation of iridium oxide requires cycling of the electrode beyond certain threshold potential limits which depend somewhat on the electrolyte and growth conditions [1,2]. In our electrolyte at pH 1.5, the threshold of the anodic potential limit would be greater than 0.65 V vs. Ag/AgCl. We expected, therefore, that there should be little, if any, formation of iridium oxide as a result of the electrochemical testing up to 205 days.

As discussed in Quarterly Report No 5, one cyclic voltammogram was taken on each site on Ribbon [illegible] over the potential range from -0.4V to +0.6V vs. Ag/AgCl after 34 days of soaking. Another [illegible] was taken on site 1 after 113 days of soaking (see Figure 2.5 in QPR-6). The 34 day measurements showed that there was a small amount of oxide on some of the sites. The amount of oxide was largest on site 1 and decreased in the order of site 1, site 6, site 2, and site 5. This progression is not only the order of the sites ranked by distance from site 1, but also is the order from the top of the probe closest to the electrolyte atmosphere interface down into the solution. The measurement on site 1 after 113 days showed about a 50% increase in the current attributed to oxide on the electrode. As seen in Figure 2.2, the apparent capacitance measured at 200 V/s increased about a factor of three over this period.

This quarter [illegible] voltammetry experiments were run after [illegible] days of soaking on all [illegible] rate changes [illegible] amount of oxide. The potential range covered was from [illegible] [illegible] Ag/AgCl [illegible] wider potential range was used [illegible] provide more details of the [illegible] oxide film. The scan rate was 100 mV/s, twice the rate used for the [illegible] for the six sites are shown in Figures 2.3 through 2.5. The CVs for [illegible] wider potential range taken after 34 days of soaking are also plotted. The [illegible] the earlier CVs have been multiplied by two to account for their being measured at [illegible] the scan rate used this quarter.

[illegible] three categories, each of which provides interesting and different [illegible] The CVs for sites 3 and 4 shown in Figure 2.5 are plotted on a 0.1 nA div scale [illegible] sensitive than used for the other sites. Site [illegible] continued to behave as a [illegible] resistor with high resistance rather than a metal showing electrochemical behavior.

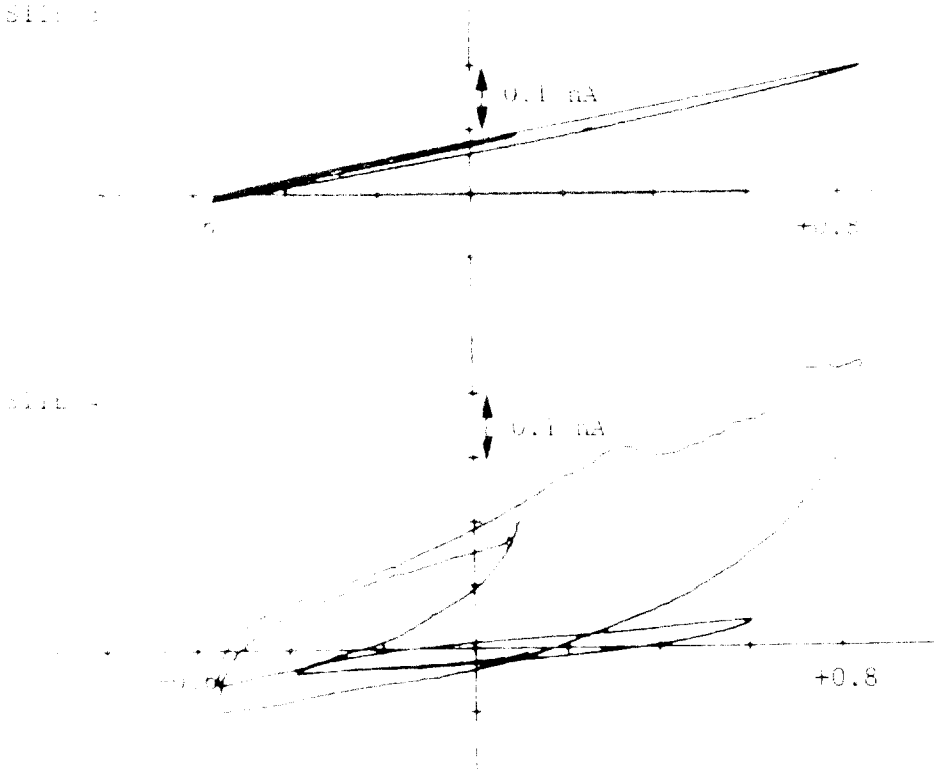

[illegible] of site 3 (top) and 4 (bottom) of the U. Michigan ribbon cycle [illegible] after [illegible] days of passive soaking. For comparison, the results after 34 days [illegible] barely distinguishable on x axis for site 3 multiplied by two to [illegible] the different sweep rate (see text). Measurements made in deaerated [illegible] rate of 0.1 V/s. Potentials are referenced to Ag/AgCl.

The current is higher than after 54 days, is tilted and offset in the anodic direction. The CV of site 4 has [illegible] characteristics except that there are some small peaks associated with electrochemical reactions and the CV has a wider envelope. There appears to be a larger area of site 4 in contact with the electrolyte than site 5.

The CVs shown in Figure 2.4 for sites 6, 2, and 5, listed in order from site 1, form another set of CVs with common properties. One of the most important features is that the current at 0.0 V vs. Ag/AgCl on the positive going sweep for site 6 and 2 has not changed over the 145 day soaking period. There has therefore been little if any degradation of the seal between the insulator and the metal over the 145 day soaking period. The slightly higher current on site 5 [illegible] in the CV and the anodic current at the initiation of the CV all reflect a slightly [illegible] but still quite stable insulator/metal seal. Site 2 has the least tilted CV and the initial current is the anodic properties of a metal electrode with a good insulator/metal seal. Site 6 has a sharp anodic peak at 0.16V vs. Ag/AgCl which was also observed on site 1 (see Figure 2.5). There was no corresponding cathodic peak. The anodic peak disappeared on the second [illegible] cycle. The peak is probably due to some electroactive species absorbed on the electrode surface.

All three sites show electrochemical peaks in the anodic sweep associated with iridium oxide. The current in this region has increased over a factor of two during the soaking period. These measurements support our assertion, therefore, that the increase in the capacitance observed on site 1 is due more to oxide growth than to an increase of the geometric area of the electrode site.

The CV for site 1 shown in Figure 2.5 shows a large contribution from iridium oxide. The CV [illegible] and begins with only a slightly anodic current indicating that there is still a good seal between the insulator and the metal. The charge balance is good. The charge storage capacity (CSC) from integration of the CV gives 0.016 μC and 0.017 μC for the anodic and cathodic charge, respectively, corresponding to 6.7 mC/cm² for the nominal electrode area of 500 μm². The major anodic and cathodic peak at 0.22V and 0.14V vs. Ag/AgCl, respectively, are at the right potentials. The poorly shaped anodic peak at 0.56V and less distinct cathodic peak at [illegible] the same potential are often observed in AIROF films that have been in PBS for extended

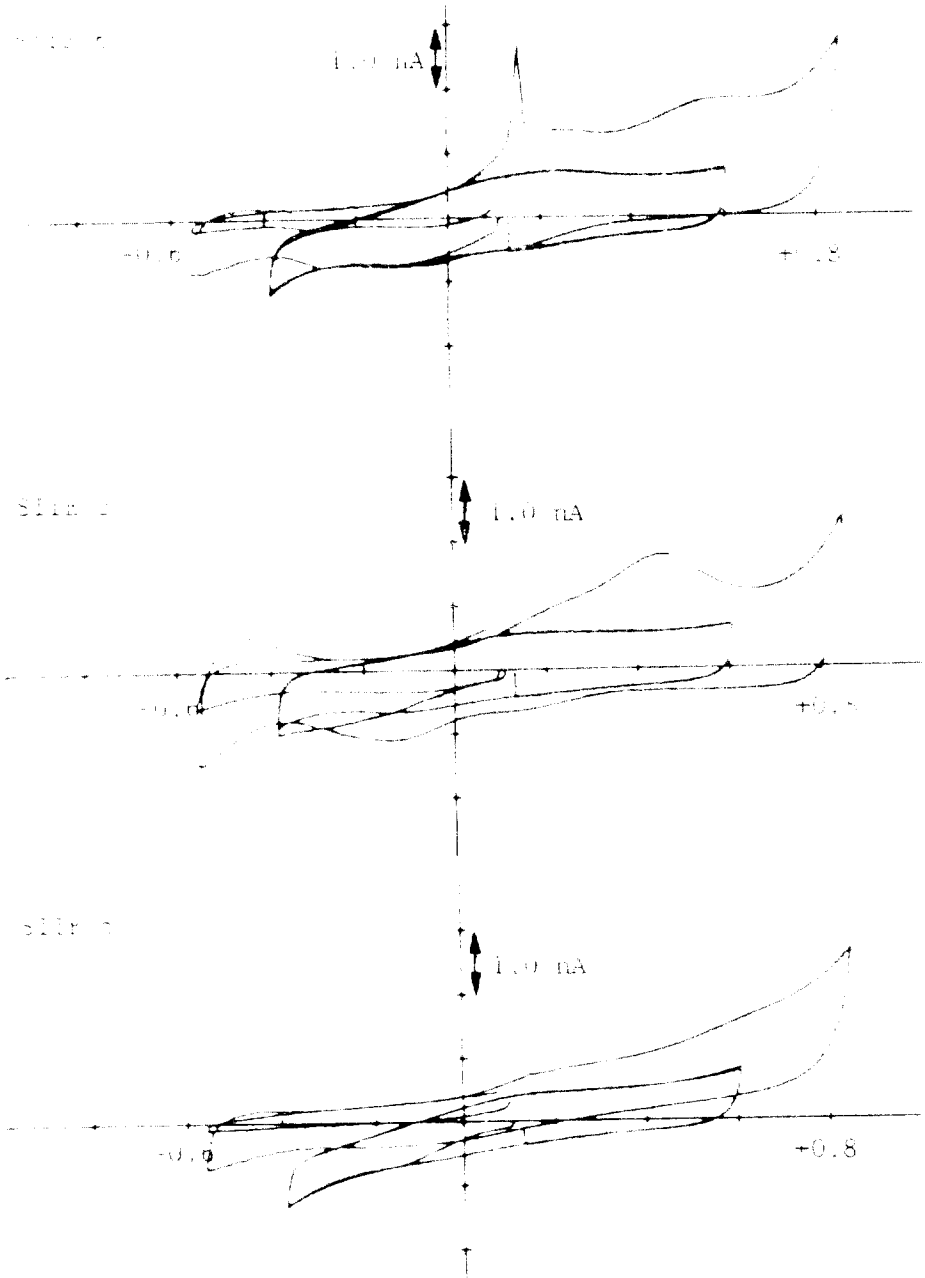

[illegible] Voltammograms of site 6 (top) and 2 (middle) and 5 (bottom) of the [illegible] Michigan [illegible] cable No. 1 after 17 days of passive soaking. Voltammograms measured [illegible] are shown for comparison. Conditions as described in Figure 2-3.

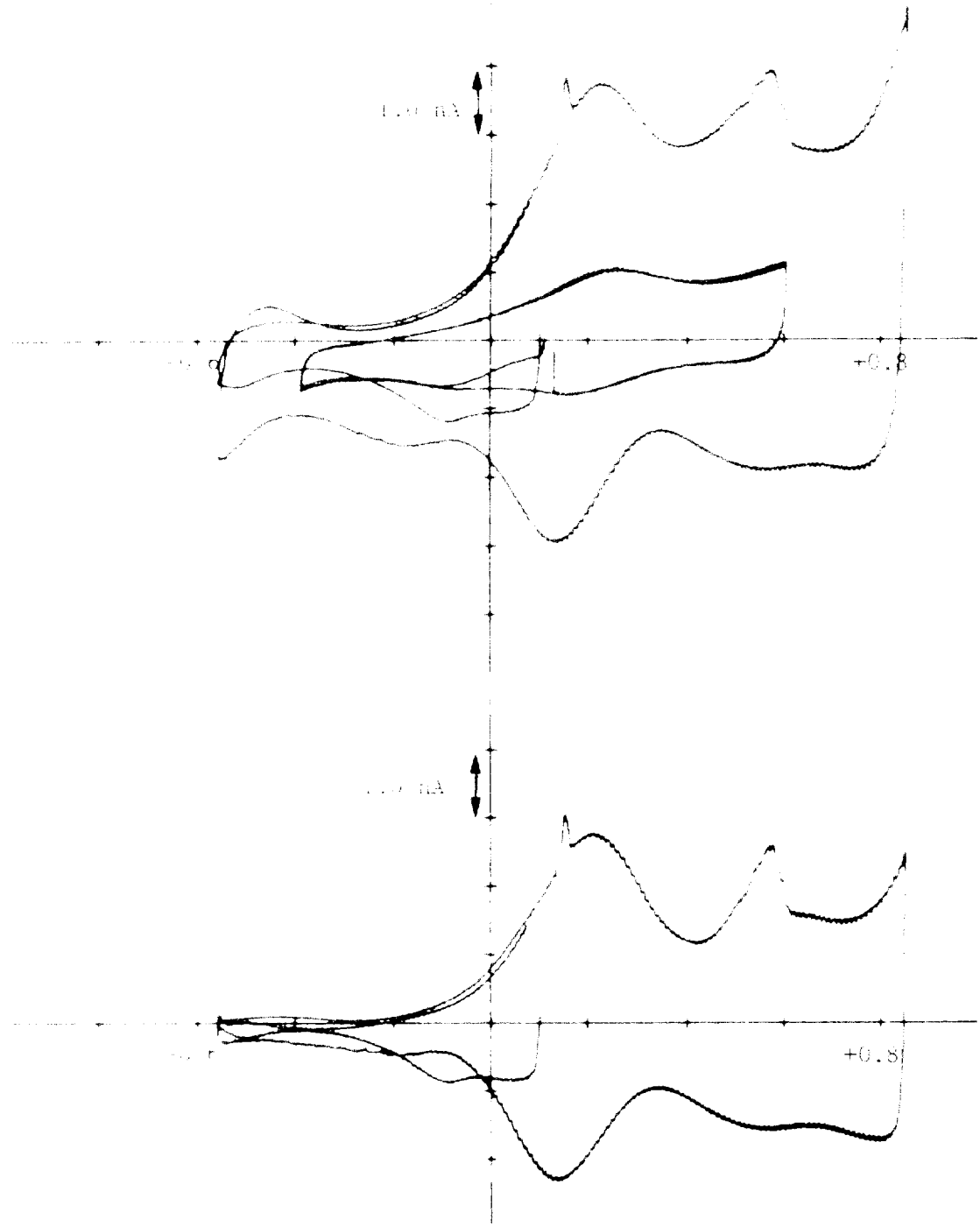

[illegible] Voltammograms of site 1 of the C. Michigan ribbon cable No. [illegible] after 171 [illegible] passive soaking. Voltammograms measured after 54 days are shown for [illegible] Bottom. Voltammogram resulting from the subtraction of the [illegible] from that on site 1. Conditions as described in Figure 2.3.

[illegible] and for iridium oxide that is activated in alkaline electrolytes. In 1 N H_2SO_4 this additional peak has been attributed to formation of $IrO_2(OH)_2$ with pentavalent iridium [3, 4]. Evidence is growing that the hydroxide ion is important in the electrochemical switching of AIROF films in H_2SO_4 along with movement of water in and out of the film [5] (see Section 3).

A [illegible] question is why there is oxide on the site since the electrochemical testing should [illegible] resulted in activation in the conventional manner. Comparison of the CV on site [illegible] with the others clearly shows that the electrochemical testing has had some effect on the on site electrode [illegible] the 200 day period. Sites 2, 6 and 5, which have been subjected to significantly less soaking, also showed increased charge in the oxide region, but the shape of the CV was [illegible] different. The CV of site 2 shown in Figure 2.4 exhibits a broad anodic and cathodic peak separated by about 0.6V. The potential halfway between the two peaks is 0.16V vs. Ag/AgCl, which is very close to the value for the Ir^{3+}/Ir^{4+} peak. Thus the soaking of the site has led to formation of oxide that is either itself resistive or is accessed through a resistive layer. If this same process occurred at site 4 during the soaking, we can subtract the CV of site 2 from that of site 4 to remove the contribution from this "background" oxide. The result, shown in the bottom of Figure 2.5, is to remove the charge in the portion of the CV negative of -0.2V vs. Ag/AgCl and move the Ir^{3+}/Ir^{4+} peak to slightly less anodic potentials. This result is consistent with a quality AIROF film having little internal resistance which would be desirable for use of pulse stimulation. The combination with the "poorer quality" oxide found on site 2, however, might result in poorer charge injection properties in a prosthetic application.

The results of this extended soaking experiment have provided significant insight into the stability of sputtered Ir films. One conclusion is that the interface between the metal and substrate has held up extremely well. Another is that the electrochemical testing has grown some quantity of oxide compared to the simple soaking which leads to an increase in charge capacity due to some kind of a resistive oxide. The details about formation of, or access to, this specific oxide are not known. One possibility is oxide formation on the surface of the Ir films during sputter deposition or after post deposition exposure to humid air. The columnar microstructure of the Ir films may result in difficult to access internal surfaces that may be oxide coated. These surfaces may also [illegible] during extended soaking and cycling as electrolyte penetrates into void spaces [illegible]. Another possibility is that during the soaking there is a slow formation of a

[illegible] scale of the surface which has poor electrochemical properties. In this case, it might be [illegible] the electrode shortly after it is fabricated to insure that the oxide formed had the desired electrochemical properties.

2.2.4 Michigan Ribbon-Cable Probe 4, Site 5.

A [illegible] ribbon cable probe of the Schmidt Type with Ir microelectrodes supplied by the [illegible] Michigan group was mounted for testing in the cell described in QPR 6. The goal was to characterize site 5 on this electrode with the Ru hexaammine procedure and EIS and then begin [illegible] different sites. All solutions used for the pretesting and the scan rate study were [illegible]. A cyclic voltammogram between -0.4 and +0.5 V vs. Ag/AgCl at a sweep rate of [illegible] V/s in 0.1 M PBS was done on site 5 to detect the presence of any oxide on the Ir [illegible]. The CV showed no evidence of the iridium being "activated".

Cyclic voltammograms were measured over the sweep rates from 0.001 to 200 V/s in solutions with and without Ru hexaammine dissolved in PBS on day 12. A CV over the wide potential window in PBS was taken after the scan rate study. Comparison of the cyclic voltammograms in deaerated PBS before and after the scan rate study shown in Figure 2.6 [illegible] that there was some slight "activation" of the electrode after the scan rate study, [illegible] a slight anodic and cathodic peak is evident at the widely spaced potentials observed on site 2 for ribbon No. 1 discussed above.

Table 2.2 lists the voltammetric data for the scan rate study. The data was analyzed in the manner described in QPR 6 [6]. The results are qualitatively similar to those obtained previously [illegible] electrodes with rectangular sites nominally 15 x 38 μm (500 μm²). As we [illegible] characterizations of electrodes of this type, the results measured at scan rates above [illegible] V/s could not be used because of the large background. The background corrected voltammograms obtained from 0.001 to 0.020 V/s were sigmoidal in shape with maximum current independent of scan rate, although only the curve for a sweep rate of 0.005 V/s had coincident forward and reverse waves. The steady state current, however, was only half that obtained on the sites on Ribbon #1 and #2. The radius calculated from the analysis assuming a [illegible] of the ultramicroelectrode was 6.8 μm corresponding to an area of only 145 μm² [illegible] smaller than the nominal geometric area.

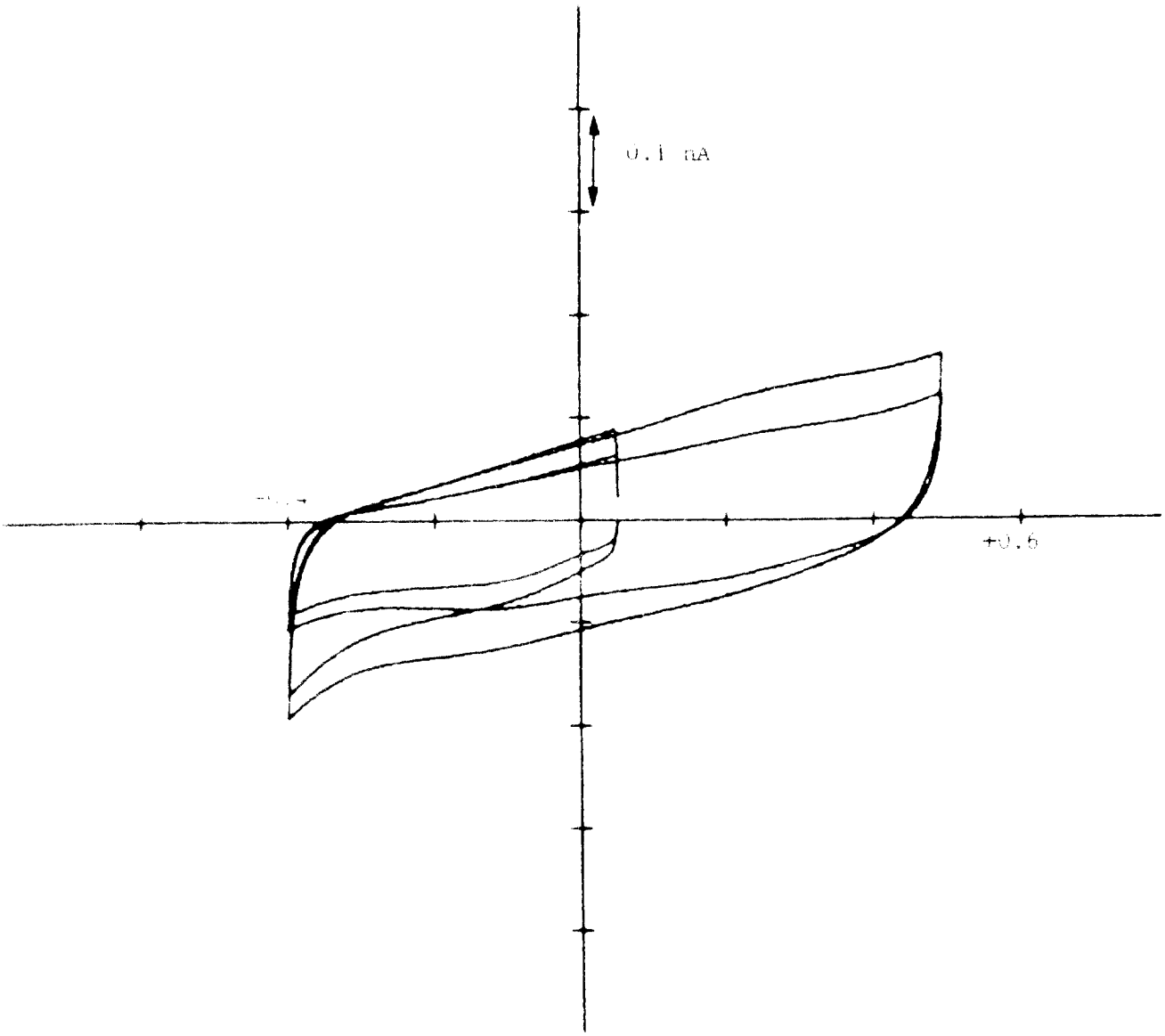

FIGURE 27 Comparison of wide potential cyclic voltammograms for U. Michigan ribbon carbon probe No. 4 site 5 before and after scan rate study. Electrolyte is deaerated 0.1 M PBS and the scan rate is 0.05 V/s. Potentials are referenced to Ag/AgCl.

Table 2.2 Data for electrochemical study 1 on site 5 of U. Michigan ribbon cable probe No. 4[a]

Scan Rate (V/s)	Half Wave Potential $E_{1/2}$ (V)	Maximum Current i_m (nA)	Current Function $i_m v^{-1/2}$ (nAV$^{-1/2}$s$^{1/2}$)	Disk Radius[b] (μm)
0.00[illegible]	[illegible]	2.20	69.6	6.4
0.002	0.20	2.45	54.8	7.0
0.005	0.2[illegible]	2.50	35.4	7.0
0.0[illegible]	0.20	2.45	24.5	6.9
0.0[illegible]	0.20	2.50	1[illegible]	6.9
0.050	0.20	2.5[illegible]	11.5	7.0
0.[illegible]	0.20	2.68	8.5	7.1
0.200	0.20	2.85	6.4	7.2

[a] Reduction of ruthenium hexaammine in a solution of 1.38 mM $Ru(NH_3)_6Cl_3$ in PBS corrected for residual and charging current in PBS alone. Potentials are vs. Ag/AgCl/3 M NaCl.
[b] Calculated from the maximum current using Eqs. (1) and (2) in QPR-6 which assumes the electrode geometry is a disc.

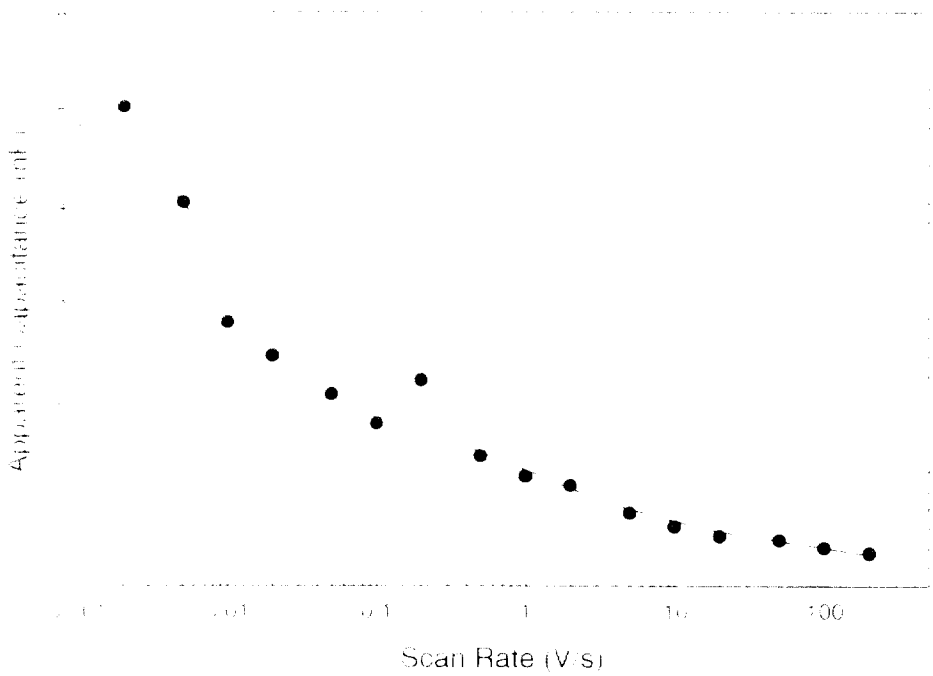

Figure 2.[illegible] Plot of C_{app} as a function of sweep rate for site 5 on ribbon No. 4 taken in PBS during the Ru study.

The apparent capacitance as a function of sweep rate is plotted in Figure 2.7. The electrochemical surface area for site 5 calculated from the apparent capacitance at 200 V/s was 1370 μm² which is similar to the value of 1590 μm² that we obtained initially on site 1 of ribbon No. 1 but only 30% of site 5 on ribbon No. 2.

After the scan rate study, a number of EIS measurements were made on site 2 of this electrode. The electrode was left in distilled water between electrochemical measurements. The cyclic voltammograms of site 2 taken regularly as part of the EIS characterization showed no unusual behavior. Forty eight days after the scan rate study, 4 days after the last CV/EIS characterizations, and just prior to our scheduled beginning of activation of the sites, cyclic voltammograms were taken in deaerated 0.1M PBS at 0.05 V/s between -0.4 and +0.2V vs. Ag/AgCl. Figure 2.8 shows the progressively more resistive behavior of site 3, a typical indicator of a leak between the metal and insulating layer. This behavior was seen at all six sites on ribbon-cable probe No. 4 and prevented any further electrochemical measurements on this probe.

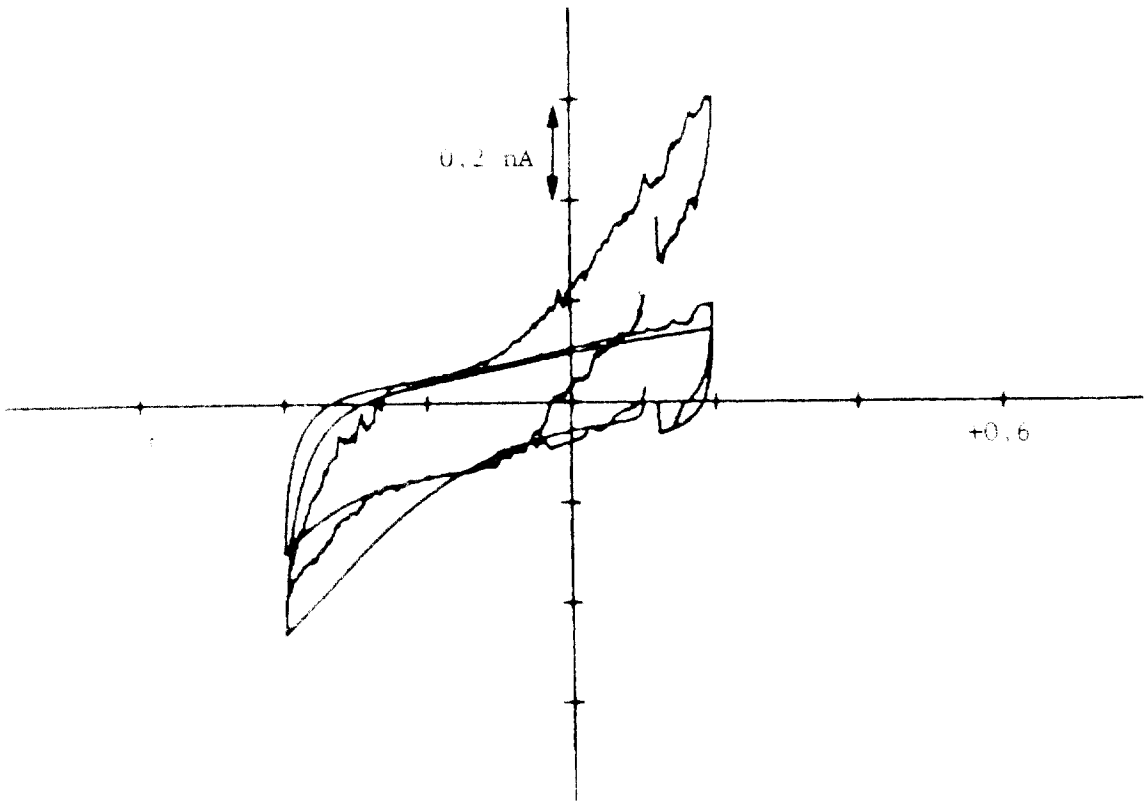

Figure 2.8 Voltammograms of 4 Michigan ribbon-cable probe no. 4 site 3 at 0.05 V/s in deaerated 0.1M PBS after 60 days soaking. Potentials are vs. Ag/AgCl/3 M NaCl.

Table 2.3 Comparison of dimensions determined from electrochemical testing of sputtered iridium electrodes of Schmidt 2 type on U. Michigan ribbon cable probes.[1]

Electrode Site / Ru Study No.	Days leaked	Ru Conc. (mM)	i_L (nA)	radius disk (μm) SS[2]	radius disk (μm) Aoki[3]	ESA (μm) SS	ESA (μm) Cap	ESA (μm) Cap/SS	Status
Ribbon cable #1 site 1 study	[illegible]	1.38	4.8	13.5	[illegible]	572	5590	2.3	OK 205 d
Ribbon cable #2 site 2 study	[illegible]	1.34	4	13.4	13.5	565	4560	8.1	OK 10 d
Ribbon cable #4 site 3 study	[illegible]	1.38	2.5	6.2	6.9	132	370	10.4	leaked 60 d

[1] Nominal electrode dimensions were 13 x 38 μm for a geometric area of 500 μm.
[2] Radius and area calculated from steady state current at the lower scan rates (6).
[3] Calculated from current function at low scan rates using Aoki equation (6).
[4] Area determined from apparent capacitance based on background current at 200 V/s scan rate and 25 μF/cm² for iridium.

Table 2.3 compares the results of the electrochemical measurements on sites of three different ribbon cables we have evaluated with the Ru technique and fast CVs. The comparison shows that the site on Ribbon No. 1 and Ribbon No. 4 had comparable areas as measured by the capacitance method, whereas the areas for the site on Ribbon No. 1 and No. 2 were similar from the Ru analysis. The much longer stability of the site on Ribbon No. 1 compared to that on Ribbon No. 4 may show that the small value for the area measured by the Ru analysis presages the resulting instability. Another possibility is that the ratio of the area determined by the capacitance and the steady state values may predict the long term stability of the electrode. The absolute values may not be as useful as the ratio since we have shown that the measurement of the current at 0.0 V vs. Ag/AgCl on which the apparent capacitance is measured is influenced by the amount of Ru dc present. Unfortunately, Ribbon No. 2 was broken after the 10th day so that long-term soaking information was not obtained to support this theory. Measurements on additional electrodes are necessary to determine if either of these correlations can be used in predicting electrode stability.

3. ELECTRODES WITH GRADED Ti-Ir INTERFACES

This quarter we began studies of new materials and fabrication procedures to permit stimulation at high charge densities by looking at methods for enhancing the adhesion and mechanical stability of electrode materials sputtered onto conductive substrates. Since Ti is frequently used as the interlayer between polysilicon conductors and sputtered Ir metal [7, 8], the work focused on Ti-Ir bilayers. The increase in volume when Ir is electrochemically activated to form $SIROF$ (a hydrated Ir oxide) is about a factor of ten. Such large dimensional changes cannot be readily accommodated at interfaces. Overactivation of comparatively thick Ir films [illegible] can lead to mechanically unstable structures that are susceptible to spalling while activation of the Ti-Ir interface of thinner Ir films will lead to delamination. These mechanisms have been identified as reasons for failure of thin film stimulation electrodes. To avoid the formation of $SIROF$ when the activation reaches the discrete Ti-Ir interface, the use of compositionally grading between the Ti and Ir films is being investigated.

3.1. Preparation of Ti-Ir Films by Sputter Deposition

The Ti and Ir are deposited by DC sputtering using a multitarget apparatus that allows sequential or simultaneous sputtering from independently controllable sputtering guns. The apparatus is shown schematically in Figure 3.1. As many as four sputter guns, two are shown in Figure 3.1, are chosen from a 40 cm diameter flange along with the substrate holder. Computer control of the sample holder switches the substrates between targets to form discrete multilayers or rotates them to form alloy films. The rotation speed is 105 rpm which results in less than a monolayer deposition on each pass for deposition rates of 15 nm/min or less. To make the compositionally graded Ti-Ir interfaces, the current to the individual sputter guns was raised or lowered while maintaining a total sputtering current of 150 mA throughout the deposition. A typical current versus time profile for depositing a Ti-Ir graded interface electrode is shown in Figure 3.2.

Figure [illegible] Schematic diagram of sputter deposition apparatus used to produce graded interfaces in multilayer thin films

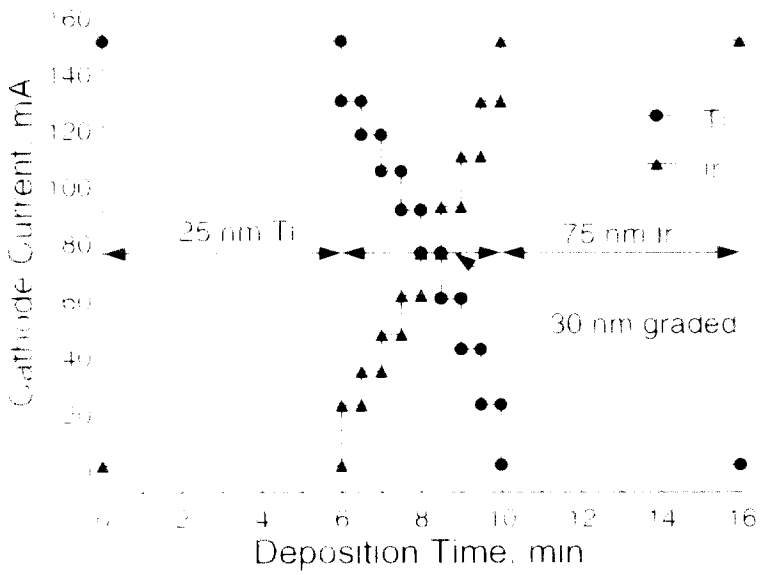

Figure [illegible] Cathode versus time profile used to grade the composition of the interface between [illegible] and [illegible] a Ti/Ir electrode on Si

Table 3.1 Conditions for sputter deposition of Ti and Ir films with discrete and graded interfaces on silicon

Base pressure	2.0×10^{-7} torr
Sputter gas and flow rate	Ar, 40 sccm
Sputter gas pressure	10 millitorr
Power	Ti target voltage 530 V at 150 mA Ir target voltage 500-600 V at 150 mA
Target to substrate distance	6.2 cm
Temperature	ambient (25 °C)

~25 nm Ti adhesion layer is first deposited on the Si as an adhesion layer. The graded layer, approximately 90 nm thick, is then deposited followed by a 75 nm layer of pure Ir. The deposition rates of the Ti and Ir were estimated from surface profilometer and scanning electron microscope measurements. For films sputtered at 150 mA, the deposition rates were 4 nm/min and [illegible] nm/min for Ti and Ir respectively. The deposition conditions for the Ti and Ir are listed in Table 3.1.

Film thickness measurements and compositional depth profiling of graded and discrete interface electrodes using Auger spectroscopy revealed that the transition from Ir-rich to Ti-rich layers in the graded region was more abrupt than intended. Since the deposition rate of Ir was [illegible] times that of Ti, the current time profile favors Ir rich compositions in the graded layer. The steeper gradient arose because the current time profile shown in Figure 3.2 used for the composition grading was developed prior to accurate measurements of Ti and Ir deposition rates.

3.2. Electrochemical Test Protocol

Initial experiments focused on relatively thin Ir films (~75 nm) to allow complete activation of the Ir in a convenient time. Electrodes with an area of 0.01-0.02 cm² were made by masking an approximately circular area of the sputtered films with epoxy. Electrodes were activated using our established pulsing protocol in 0.8M Na_2HPO_4 (pH 9.2) or in phosphate buffered saline (PBS) (pH 7.4). The results of activation of a discrete interface Ti-Ir electrode [illegible] in 0.8M Na_2HPO_4 using square pulses 0.5 s wide between potential limits of -0.8

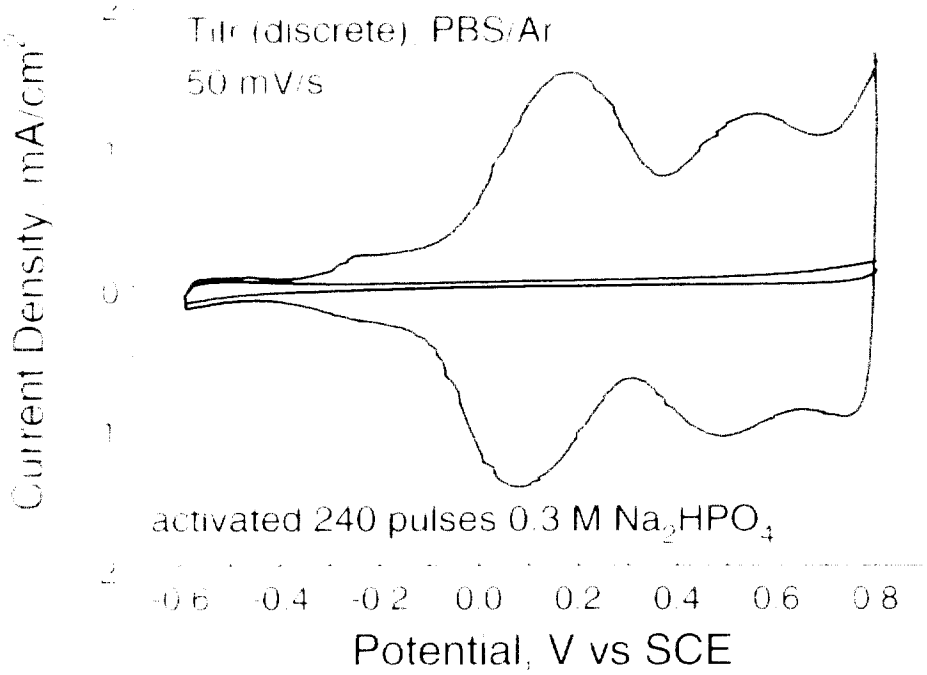

Figure [illegible] Cyclic voltammogram of discrete interface Ti/Ir electrode in Ar sparged PBS, before and after 240 activation pulses in 0.3M Na_2HPO_4.

[illegible] vs. SCE for 240 pulses are shown in Figure [illegible]. The cyclic voltammograms were taken in Ar sparged PBS at 50 mV/s between limits of -0.6 and 0.8V vs. SCE immediately before and after activation. The 240 pulse activation resulted in a charge capacity at this sweep rate of [illegible] for both the cathodic and anodic half-cycles of the voltammogram, indicating excellent charge balance. Similar activation behavior was observed for electrodes with graded interfaces.

[illegible] activation, discrete and graded interface electrodes were pulsed potentiostatically between potential limits that were gradually increased to promote activation of [illegible]. It was necessary to increment the potential limits to avoid oxygen bubble formation that would damage the electrode surface if the pulsing at higher potential limits was initiated immediately after the electrode was activated. Cyclic voltammograms were recorded after pulsing in each potential range. The CVs were taken between limits of -0.6 and 0.8V vs. SCE at a sweep rate of [illegible] in the same Ar sparged PBS electrolyte.

3.3. Electrodes with Discrete Ti-Ir Interface and 75 nm Ir Films

The potential limits and number of pulses at each limit and charge capacity are listed in Table 5.2 for an electrode with a discrete Ti-Ir interface and a 75 nm film of Ir. Figure 5.4 shows selected voltammograms recorded during the 11520 pulses on the electrode. Activation of the electrode was based on the first 5840 pulses between a maximum potential range of -0.75 to 0.9 V vs. SCE. The charge capacity increased from 18 mC/cm² to 42 mC/cm², and the charge in the anodic and cathodic halves remained balanced. There were no significant changes in the shape of the voltammograms.

Further pulsing was done with the anodic potential above 0.90V vs. SCE. At these higher potentials, iridium oxide dissolves in 1.0N H_2SO_4, but it has not been shown that a similar dissolution occurs in neutral solutions. With the continuous pulsing, the reduction wave negative of 0.25V vs. SCE appeared to broaden and a shoulder developed at -0.25V. Between 7,680 and 9,600 cycles, the previously small anodic peak at about 0.55V vs. SCE grew significantly relative to the peak at 0.25V. On the cathodic sweep, there was little change in the current between 0.4 and 0.5V. But at more negative potentials the current decreased. The growth of the peak at 0.55V vs. SCE therefore does not appear to involve a reversible reaction. After 11,520 pulses,

Table 5.2 Results from pulse testing of an electrode (No. 052190[7]) with a discrete interface between the Ti and a 75 nm Ir film[1]

Potential vs. SCE	Electrolyte	Pulses[2]	Total Pulses	Cath. Charge mC/cm²	Anod. Charge mC/cm²
[illegible]	0.5 M Na_2HPO_4 (pH = 9.2)	240		19.4	
[illegible]	PBS (pH = 7.4)	0	0	18.0	18.3
[illegible]	PBS (pH = 7.4)	1920	1920	34.5	34.8
[illegible]	PBS (pH = 7.4)	1920	3840	42.1	42.4
[illegible]	PBS (pH = 7.4)	1920	5760	56.6	57.1
[illegible]	PBS (pH = 7.4)	1920	7680	75.9	76.6
[illegible]	PBS (pH = 7.4)	1920	9600	69.2	70.1
[illegible]	PBS (pH = 7.4)	1920	11520	48.5	49.0

[1] Electrodes activated in 0.5 M Na_2HPO_4 and then pulsed in PBS with 1 Hz square wave.
[2] [illegible] pulses at the potential limits indicated.
[3] [illegible] cathodic and anodic half of the CV measured at 50 mV/s in PBS.

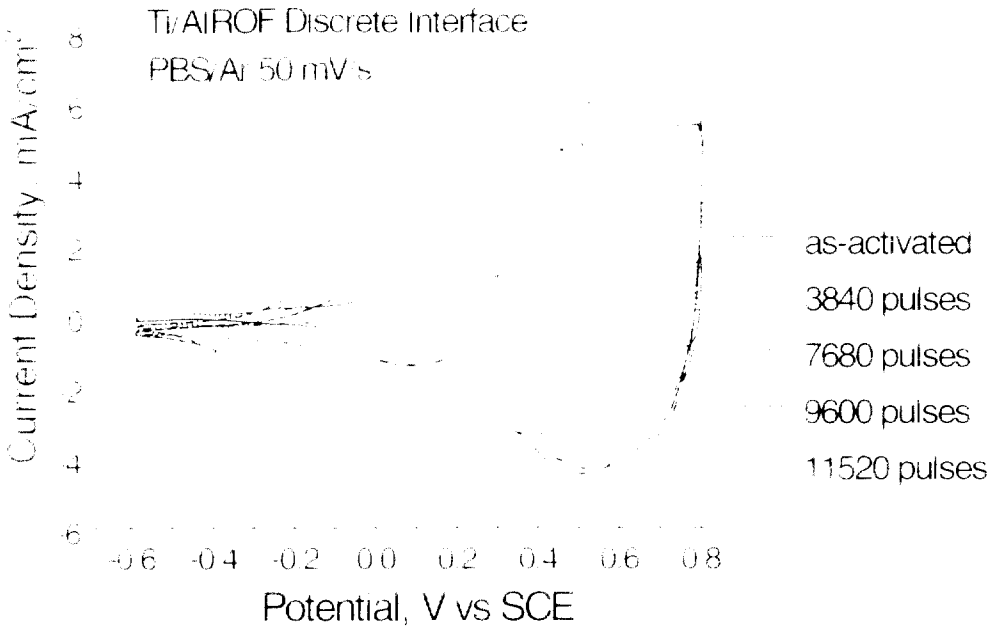

Figure 3.4 Cyclic voltammograms of discrete interface Ti/Ir electrode (75 nm Ir) taken while the electrode was pulsed over 11,520 pulses in Ar sparged PBS (see Table 3.2).

The [illegible] peak was the only prominent feature in the anodic portion of the voltammogram. Again its increased current did not have a major effect on the cathodic portion of the voltammogram in the region between 0.4 to 0.8V vs. SCE, but the current negative of 0.4V was distinctly reduced. Delamination of the AIROF was observed at 11,760 pulses.

Scanning electron microscopy of delaminated AIROF electrodes showed two distinct film morphologies. Figure 3.5 shows the cross section of delaminated AIROF from a discrete interface electrode (No. 0521968) which was activated for 10,560 pulses in PBS without initial activation in 0.3M Na_2HPO_4. The outer layer comprised a thin, ~100 nm thick, crust with no [illegible] structural features. This layer formed during the early stages of pulsing, [illegible] over the first 1,920 pulses between limits of -0.7V and 0.85V vs. SCE. The inner layer, ~400 nm thick, showed a distinct columnar morphology, indicative of lower density AIROF. The two layer structure is also revealed in the surface morphology shown in Figure 3.6. Discrete interface AIROF electrodes which were initially activated in PBS rather than 0.3M Na_2HPO_4 [illegible] over similar pulse/potential protocol. Electrodes activated in either PBS or Na_2HPO_4 [illegible] stable two layer structure.

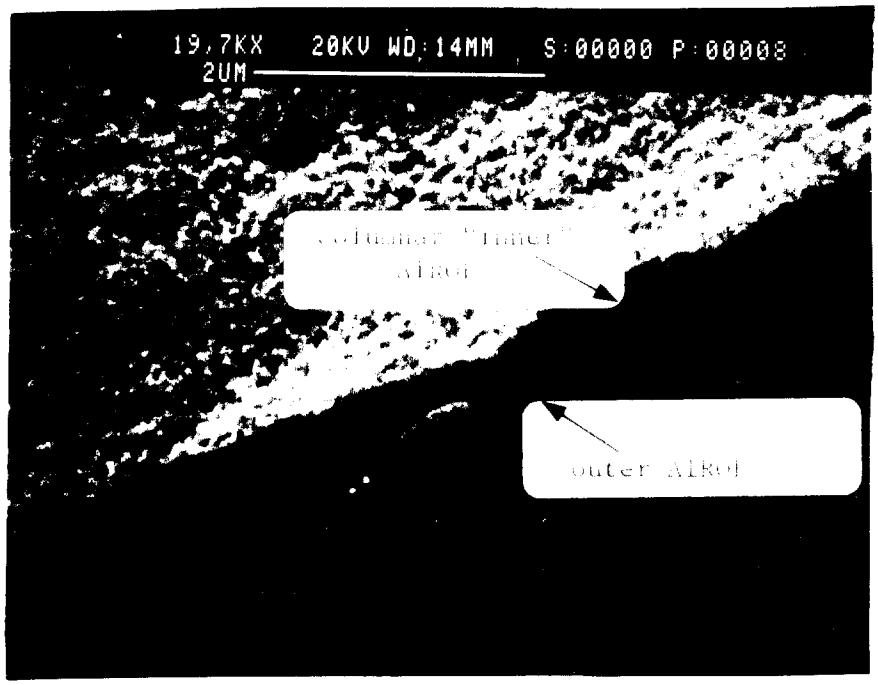

Figure 3.5 SEM cross-section of AIROF delaminated after pulsing a discrete interface Ti-Ir electrode for 11,520 pulses (see Table 3.2). Original Ir thickness was 75 nm.

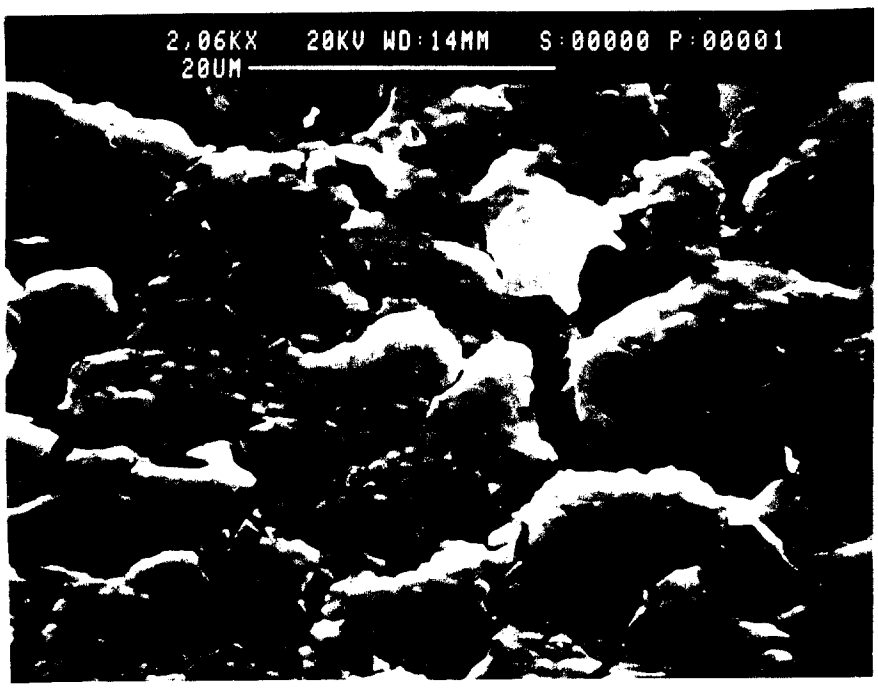

Figure 3.6 SEM of AIROF surface after delamination following pulsing of a discrete interface Ti-Ir electrode for 11,520 pulses (see Table 3.2).

Several features of the AIROF films are noteworthy. First, the AIROF delaminated at the edges of the electrode and the delamination migrated towards the center as activation continued. This progression of delamination is expected from the nonuniform current distribution during pulsing. Second, the intact AIROF had a pebble-like surface morphology, each pebble being approximately circular with a diameter of [illegible] μm. Third, the pebble-like structure mimicked granular regions of the underlying Ti film. Qualitative compositional analysis using the energy dispersive spectrometer (EDS) on the SEM indicated delamination occurred at the Ti-Ir interface. There was no Ir detected on the substrate where delamination had occurred, including the granular regions of the Ti, and no Ti was found in the delaminated AIROF. Based on the SEM measurements of the film thickness, activation of the Ir under the pulse conditions listed in Table [illegible] resulted in a [illegible]% increase in volume.

3.4 Electrodes with Graded Ti-Ir Interface and 75 nm Ir Films

The activation data for a graded interface Ti-Ir electrode deposited with a time-current profile shown in Figure [illegible] are listed in Table [illegible]. The graded interface electrode was pulsed [illegible] times before delamination at the edges of the electrode was observed. The increase in charge as the electrode was activated followed that obtained on the electrode with the discrete interface up to [illegible] 680 pulses. Continued pulsing lead to an increase in charge on the electrode with the graded interface up to 13,540 pulses whereas it began decrease after 7680 pulses for the discrete interface electrode. Moreover, after reaching the maximum charge, the charge decreased much less slowly for electrodes with the graded interface.

The CVs are compared in Figure [illegible] for the initial, as activated condition, after 13,540 pulses [illegible] at the maximum charge capacity, and after delamination. The cyclic voltammograms show the same two primary features observed with the discrete interface electrodes. Both the cathodic wave at 0.25 V vs. SCE and the anodic wave at 0.55 V vs. SCE decreased. There is an anodic peak at 0.15 V vs. SCE evident in the CV at the maximum charge which might be associated with the cathodic peak at 0.25 V. An electrode with a graded interface which was activated only by pulsing in PBS exhibited similar behavior with regards to charge, change in cyclic voltammetry, and delamination.

Table [illegible] Results from pulse testing of an electrode (No. 0522906) with a graded interface between the Ti and a [illegible] nm Ir film[a]

Electrolyte	Pulses	Total Pulses	Cathodic Charge (mC/cm²)	Anodic Charge (mC/cm²)
[illegible] M Na HPO, pH = 9.25	240		[illegible]	[illegible]
PBS (pH = [illegible])	0	0	[illegible]	[illegible]
PBS (pH = [illegible])	1920	1920	[illegible]	29.5
PBS (pH = [illegible])	1920	3840	[illegible]	37.6
PBS (pH = [illegible])	1920	5760	[illegible]	38.0
PBS (pH = [illegible])	1920	7680	[illegible]	62.8
PBS (pH = [illegible])	1920	9600	[illegible]	77.6
PBS (pH = [illegible])	1920	11520	[illegible]	82.0
PBS (pH = [illegible])	1920	13440	[illegible]	83.4
PBS (pH = [illegible])	3840	17280	[illegible]	[illegible]
PBS (pH = [illegible])	3840	21120	[illegible]	77.8
PBS (pH = [illegible])	19200	40320	[illegible]	[illegible]

[a] Electrodes activated in 0.5 M Na HPO, and then pulsed in PBS with [illegible] square wave [illegible] pulses at the potential limits indicated.

[b] [illegible] the cathodic and anodic half of the CV measured at 50 mV/s in PBS.

Scanning electron microscopy of the graded interface electrodes revealed a two-layer structure consisting of a thin, featureless outer layer about 130 nm thick and a columnar inner layer [illegible] nm thick. The AIROF on the graded interface electrode is slightly thicker than that [illegible] the discrete interface electrode because of the additional Ir used in the [illegible] coating. In contrast to the results with the discrete interface electrode, EDS detected [illegible] Ir in the underlying Ti film which remained on the substrate. Although the [illegible] grading is apparently preventing activation of all of the Ir, with the present [illegible] prolific delamination of the AIROF still occurred.

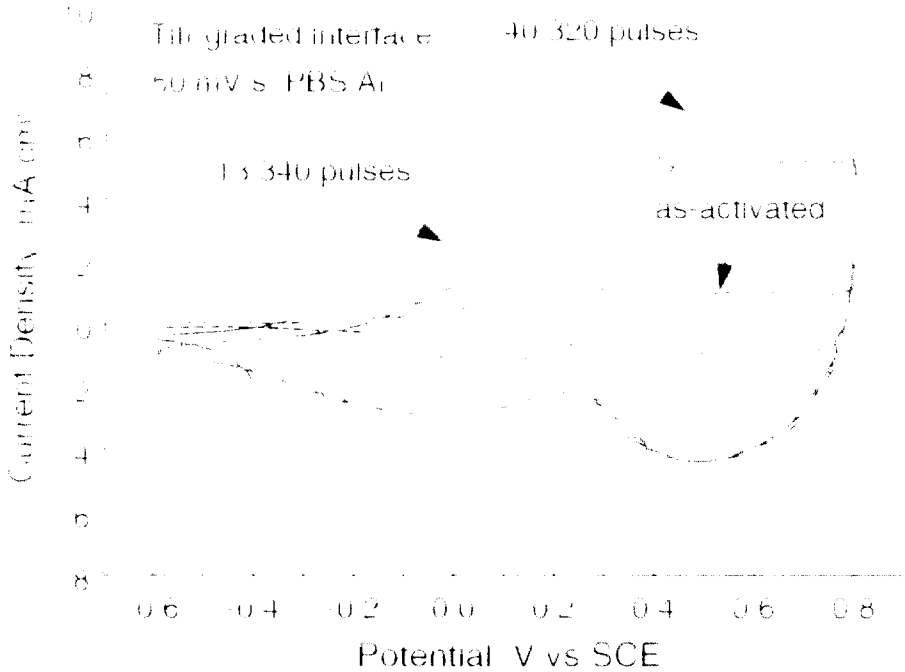

Figure 5.4 Cyclic voltammograms of a graded interface Ti/Ir electrode (75 nm Ir) over 40-320 pulses in Ar-sparged PBS (see Table 5.5).

5.5 Electrodes with Discrete Ti-Ir Interface and 100 nm Ir Films

Although over three times the number of pulses (40,000 compared to 12,000) were required to delaminate the AIROF with a compositionally graded electrode compared to that with a discrete Ti-Ir interface, the improved stability may result from the additional Ir in the graded portion of the interface. To investigate this possibility, a discrete interface electrode with a nominal Ir thickness of 100 nm rather than 75 nm was fabricated. The electrode was initially activated with 720 pulses between 0.7 V and 0.85 V vs. SCE in PBS, not 0.5M Na_2HPO_4, and then subjected to pulsing over the potential ranges shown in Table 5.4. Cyclic voltammograms are shown in Figure 5.5 after the initial activation and after delamination at 3,440 pulses (delamination). The AIROF appeared to correlate with the formation of the anodic wave at 0.67 V vs. SCE, as was observed for the graded and discrete interface electrodes with thinner Ir films.

Table [illegible] Results from pulse testing of an electrode [illegible] with a discrete interface between electrode [illegible] and a 100 nm Ir film.

Potential vs. SCE	Electrolyte	Pulses	Total Pulses	Cathodic charge (mC/cm²)	Anodic charge (mC/cm²)
[illegible]	PBS pH = [illegible]	1920		[illegible]	
[illegible]	PBS pH = [illegible]	1920	3840	[illegible]	[illegible]
[illegible]	PBS pH = [illegible]	1920	5760	[illegible]	[illegible]
[illegible]	PBS pH = [illegible]	2880	8640	[illegible]	[illegible]
[illegible]	PBS pH = [illegible]	1920	10560	[illegible]	[illegible]
[illegible]	PBS pH = [illegible]	1920	12480	[illegible]	[illegible]
[illegible]	PBS pH = [illegible]	1920	14400	[illegible]	[illegible]
[illegible]	PBS pH = [illegible]	3840	18240	[illegible]	[illegible]
[illegible]	PBS pH = [illegible]	3840	22080	[illegible]	[illegible]
[illegible]	PBS pH = [illegible]	3840	25920	[illegible]	[illegible]
[illegible]	PBS pH = [illegible]	3840	29760	[illegible]	[illegible]
[illegible]	PBS pH = [illegible]	3840	[illegible]	[illegible]	[illegible]
[illegible]	PBS pH = [illegible]	3840	[illegible]	[illegible]	[illegible]

[illegible] Pulses at the potential limits indicated.
[illegible] for cathodic and anodic half of the CV measured at 50 mV/s in PBS.

3.6 Electrochemistry of Sputtered Ir films Cycled in PBS.

[illegible] three electrodes pulsed to delamination of the AIROF are compared in Figure [illegible]. AIROF electrodes exhibited similar changes in the CV response with pulsing. [illegible] In the cathodic half cycle in a 50 mV/s CV, the anodic wave [illegible] SCE potential range begins to increase and becomes the prominent anodic wave [illegible]. Delamination was evident at the edges of the 100 nm discrete Ir and [illegible] electrodes before these CVs were acquired. The 75 nm discrete electrode had [illegible].

[illegible] shown that electrochemical reactions occur in this wave or if its increase merely [illegible] the film. The low density AIROF observed by SEM may form an [illegible] layer between the substrate and the higher density AIROF layer.

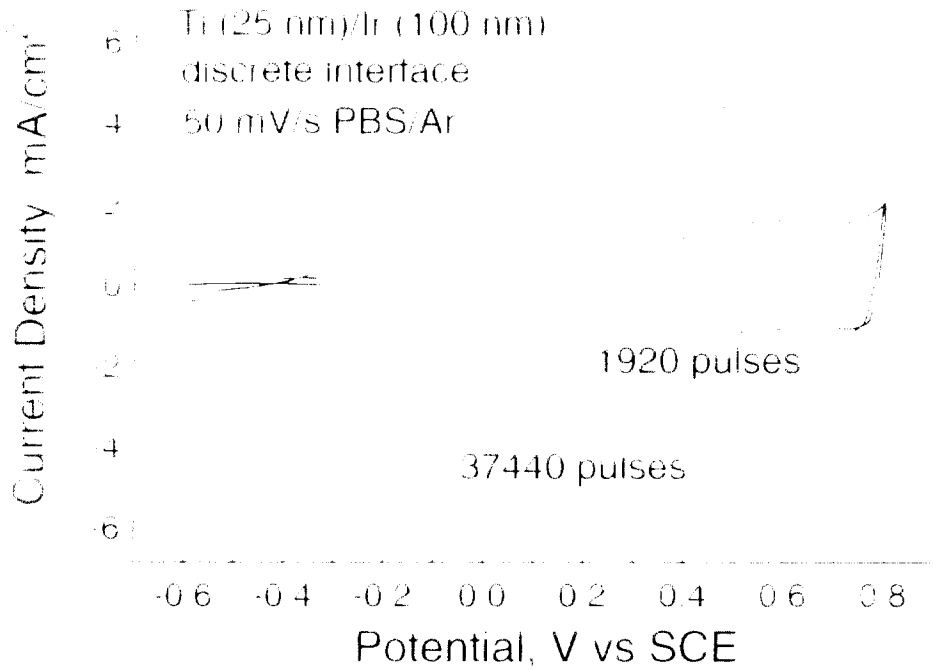

Figure [illegible] Cyclic voltammograms of a discrete interface Ti/Ir electrode (100 nm Ir) after 1920 and [illegible] 440 pulses in Ar sparged PBS (See Table [illegible])

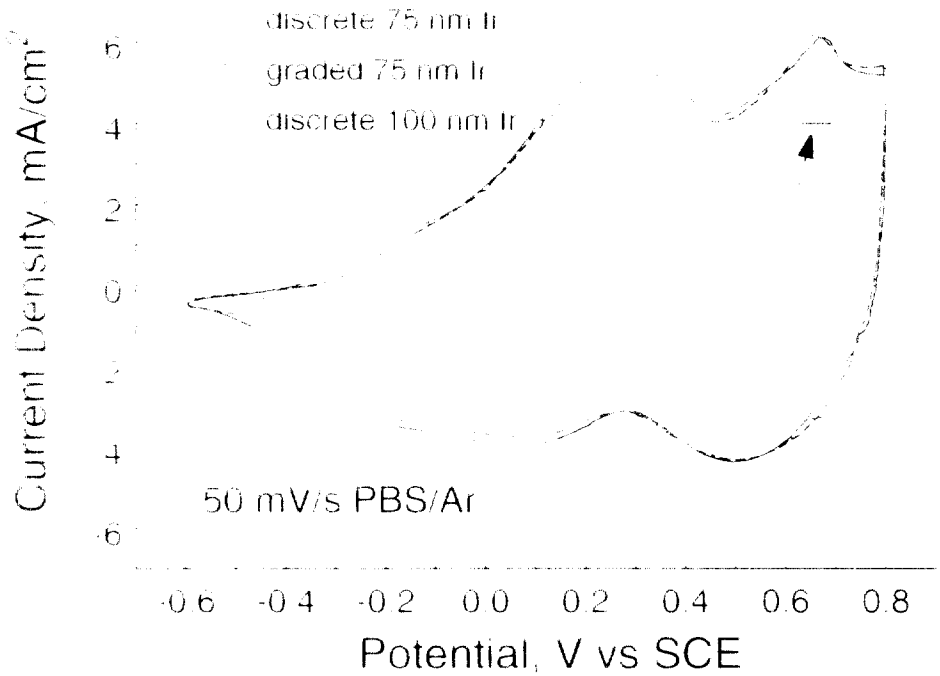

Figure [illegible] Comparison of cyclic voltammograms of Ti/Ir electrodes showing the occurrence of [illegible] at 0.[illegible] V vs. SCE associated with delamination of the AIROF

near the electrode surface. Increased charge in the 0.6 V – 0.8 V range was observed in heavily activated AIROE in acid electrolytes by Burke and Whelan (1984) who attributed the changes in [illegible] to the IrIII → IrIV oxidation [9]. The peak may also reflect increased contribution from the IrIV → IrV reaction. Finally, the peak may reflect increasing importance of the role played by the ions of the electrolyte, in this case sodium and phosphate [illegible].

There is a third wave in the potential range of -0.2V vs. SCE which grew as the activation process continued. This redox couple is most apparent by comparison of the first and second scans [illegible] as shown in Figure 5.10 for the 100 nm Ir discrete interface electrode after 18240 pulses. The -0.2 V wave appears on the second and successive CV cycles. A similar wave was also observed in a number other studies on AIROE in a range of electrolytes and film thickness. But it is not always found. The assignment of the reactions involved with this wave is not certain. Its appearance probably depends on the electrolyte and may reflect redox processes involving the electrolyte anions.

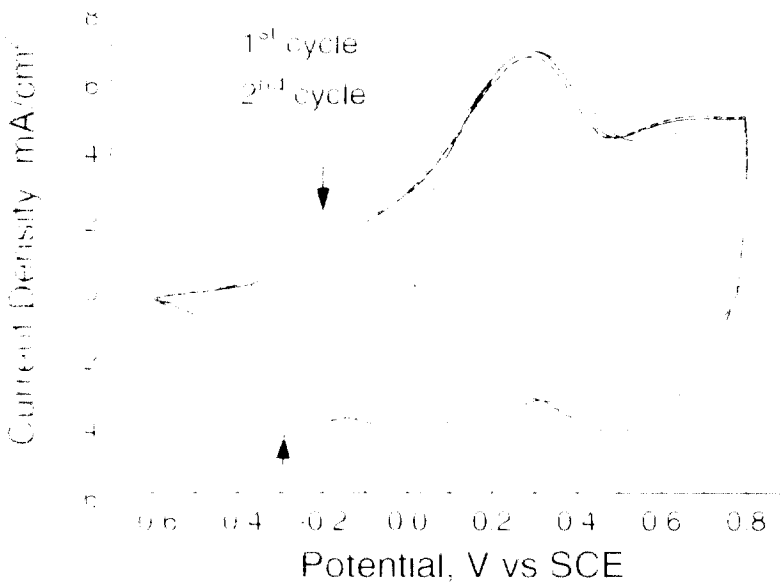

Figure 5.10 Cyclic voltammogram of AIROE showing development of a redox wave at -0.3/-0.2 V vs. SCE following 18,240 pulses in PBS/Ar

Table 3.5 Comparison of Redox Potentials of AIROF on sputtered electrodes with those grown on Ir rods measured at pH 7.5

Redox Reaction	AIROF on Sputtered Ir films (This work)[a] V vs. SCE at v = 50 mV/s		AIROF on Ir metal rods [10][b] V vs. SCE at v = 5 mV/s	
	E_{ox} (V)	E_{pc} (V)	E_{ox} (V)	E_{pc} (V)
Ir(III)/Ir(IV)	0.165	0.085	0.160	0.085
Ir(IV)/Ir(V)	0.560	0.500	0.495	0.455
preweak	0.25	0.25	0.185	

[a] Pulse activation at 0.5 s in 0.3 M Na_2HPO_4 between -0.8 and 0.75 V vs. SCE for 240 cycles.
[b] Activated by cycling in 0.5 M H_2SO_4 at 50 mV/s between -0.25 and 1.20 V vs. SCE for 150 cycles.

The work on the graded interface Ti/Ir electrodes has provided an excellent method to [illegible] the electrochemistry of AIROF grown on the sputtered films in a solution with a pH and electrolyte of relevance to *in vivo* measurement. The cyclic voltammogram of the AIROF films used in this study shown in Figure 3.3 can be compared with one of the few studies of AIROF [illegible] buffered neutral pH which was done by Yuen *et al.* [10]. They used iridium rod electrodes which were activated in 0.5M vs. H_2SO_4 by potential cycling between 1.20 and -0.25 V vs. SCE to give an oxide layer with charge capacity comparable to ours. They then cycled the [illegible] mV/s to obtain as reversible a CV as possible. The results of the potential for the electrochemical reactions are compared in Table 3.5. The agreement for the Ir(III)/Ir(IV) reaction is excellent. For the other reversible reaction at more positive potentials our values are slightly [illegible]. This comparison therefore demonstrates that we are dealing with AIROF films in the detail that our study which are comparable to those grown on bulk metal substrates.

In the past we have generally interpreted the electrochemistry of our AIROF in terms of the mechanisms that have been proposed for cycling in acidic solutions and have neglected possible effects of the amount and/or other cations that might be in the solution [11]. In this simplified case the electrochemisty of iridium oxide is probably well represented by the following reaction:

$$Ir(OH)_{0.5} \leftrightarrow IrO_2(OH)_{0.5} + xH^+ + xe \qquad (3.1)$$

As pointed out by Kozo *et al.* [5] and recently supported by Huppauff and Lengeler [4] in sulfuric acid the oxidation of the $IrOOH_2$ proceeds through a series of deprotonation steps

$$IrOOH \rightarrow IrO(OH)_2 \rightarrow IrO_2(OH) \rightarrow IrO \rightarrow IrO_2 \qquad (3.2)$$

$$+ H_2O \rightarrow$$

$$IrO(OH)_2 + 2H^+ + 2e^-$$

In this mechanism there is chemical reduction which converts the IrO_2 with the Ir^{VI} state to $IrO(OH)_2$ with the Ir^{IV} state with the accompanying oxidation of water. For our experiments in aqueous solutions with a low proton concentration the role of other cations and the anions must be considered complicating even the Ir^{III}/Ir^{IV} reaction. The following reaction is proposed for oxide in neutral aqueous solutions with Li^+ ions as the cation [12, 13]:

$$IrO_2(H_2O)_x + 2e^- + 4H_2O + M^+ \rightarrow (M^+)[H_2IrIII]oxide(H_2O)_x + 4OH^- \qquad (3.3)$$

From the comparison of the cyclic voltammograms with Li^+ ions in $LiClO_4$ aqueous solutions buffered at pH 9 with 0.01M $Na_2B_4O_7$ they were able to show that there were two sets of peaks associated with the $Ir^{IV} \leftrightarrow Ir^{III}$ reaction: one a nearly reversible, pH independent, reaction at $E_{1/2} = 0.35$ V vs. SCE attributed to the Li^+ exchange (expulsion during oxidation and insertion during reduction) and another, highly irreversible reaction by proton insertion for the reduction at $E_{pc} = 0.35$ V vs. SCE and proton expulsion during the oxidation at $E_{pa} = 0.95$V.

The implication for Equation (3.3) is that not only do anions move in an out of the film during cycling but so do water molecules. This suggestion has been supported by studies on AIROF electrodeposited Ir films using a quartz crystal microbalance (QCMB) to follow the weight changes accompanying the oxidation and reduction reaction [5]. In borate/phosphate buffered solutions with pH 8.4 the mass changes increased with oxide reduction but the weight gain was not as high, with a mole of H^+ or H_3O^+ being injected for each mole of Ir reduced as expected from the simple mechanism shown in Equation (3.1) [14]. Several possibilities to explain the results were suggested all involving mechanisms involving movement of water molecules in and out of the film along with anions and cations.

The graded interface studies coupled along with the EIS measurements are beginning to provide information on changes in AIROF films which occur in neutral solutions that is important to understanding their long term operation and stability *in vivo*.

5. REFERENCES

1. Pickup, P. G. and W. I. Birss, "A model for anodic hydrous oxide growth at iridium," *J. Electroanal. Chem.*, vol. 220, pp. 83-100, 1987.

2. Conway, B. E. and J. Mozota, "Surface and bulk processes at ozidized iridium electrodes-II. Conductivity-switched behaviour of thick oxide films," *Electrochimica Acta*, vol. 28, pp. 9-[illegible], 1983.

3. Kotz, R., H. Neff, and S. Stucki, "Anodic iridium oxide films. XPS-studies of oxidation state changes and O_2 evolution," *J. Electrochem. Soc.*, vol. 131, pp. 72-77, 1984.

4. Huppauff, M. and B. Lengeler, "Valency and structure of iridium in anodic iridium oxide films," *J. Electrochem. Soc.*, vol. 140, pp. 598-602, 1993.

5. Birss, V. I. and H. Elzanowska, "Quartz crystal microbalance measurements during oxidation/reduction of hydrous Ir oxide electrodes," *J. Electroanal. Chem.*, vol. 318, pp. [illegible], 1991.

6. Twardoch, J. M., "Integrity of ultramicrostimulation electrodes determined from electrochemical measurements," *J. Applied Electrochem.*, vol. 24, pp. 835-857, 1994.

7. Anderson, D. J., K. Najafi, S. J. Langhe, D. A. Evans, K. L. Levy, J. F. Hetke, X. Xue, J. J. Zappia, and K. D. Wise, "Batch fabricated thin film electrodes for stimulation of the central auditory system," *IEEE Trans. Biomed. Eng.*, vol. 36, pp. 693-704, 1989.

8. Kovacs, G. T. A., C. W. Storment, and S. P. Kounaves, "Microfabrication of heavy metal ion sensors," *Sens. Actuators B*, vol. B39, pp. 41-47, 1995.

9. Burke, L. D., and D. P. Whelan, "A Voltammetric Investigation of the Charge Storage Reactions of Hydrous Iridium Oxide Layers," *J. Electroanal. Chem.*, vol. 166, 121-141, 1984.

10. Yuen, M. F., I. Lauks, and W. C. Dautremont-Smith, "pH dependent voltammetry of iridium oxide films," *Solid State Ionics*, vol. 11, pp. 19-29, 1983.

11. Robblee, L. S., and J. L. Rose, "Electrochemical guidelines for selection of protocols and electrode materials for neural stimulation," in *Neural Prostheses: Fundamental Studies*, W. F. Agnew and D. B. McCreery, Eds. Englewood Cliffs, NJ: Prentice Hall, 1990, pp. 25-[illegible].

12. Pickup, P. G. and V. I. Birss, "The electrochemistry of iridium oxide films in some nonaqueous solvents," *J. Electrochem. Soc.*, vol. 135, pp. 41-45, 1988.

13. Pickup, P. G. and V. I. Birss, "The influence of the aqueous growth medium on the growth rate, composition, and structure of hydrous iridium oxide films," *J. Electrochem. Soc.*, vol. [illegible], pp. [illegible], 1988.

14. Birss, V. I., personal communication.